

# Effective Potential and Interdiffusion in Binary Ionic Mixtures

M. V. Beznogov<sup>1</sup> and D. G. Yakovlev<sup>2</sup>

<sup>1</sup>*St. Petersburg Academic University, 8/3 Khlopina Street, St. Petersburg 194021, Russia*

<sup>2</sup>*Ioffe Physical Technical Institute, 26 Politekhnicheskaya, St. Petersburg 194021, Russia*

(Dated: August 16, 2018)

We calculate interdiffusion coefficients in a two-component, weakly or strongly coupled ion plasma (gas or liquid, composed of two ion species immersed into a neutralizing electron background). We use an effective potential method proposed recently by Baalrud and Daligaut [PRL, **110**, 235001, (2013)]. It allows us to extend the standard Chapman-Enskog procedure of calculating the interdiffusion coefficients to the case of strong Coulomb coupling. We compute binary diffusion coefficients for several ionic mixtures and fit them by convenient expressions in terms of the generalized Coulomb logarithm. These fits cover a wide range of plasma parameters spanning from weak to strong Coulomb couplings. They can be used to simulate diffusion of ions in ordinary stars as well as in white dwarfs and neutron stars.

## I. INTRODUCTION

The importance of Coulomb ionic mixtures cannot be understated in many fields of physics and astrophysics. In astrophysics, dense Coulomb plasmas are encountered in neutron star crusts (e.g. Refs. [1–4]), in white dwarfs (e.g. Refs. [5–10]), and in giant planets (e.g. Ref. [11]). Similar properties possess also dusty plasmas (e.g. Ref. [12]) with numerous applications in science and technology. The properties of dense Coulomb plasmas are also important for inertial confinement fusion (e.g. Ref. [13]), antimatter (e.g. Ref. [14]), and ultra cold plasmas (e.g. Ref. [15]). Many applications of such plasmas involve diffusion.

To describe ion diffusion in Coulomb plasmas one needs the expressions for the diffusion currents and diffusion coefficients. The first problem was addressed in our previous work [16]. The second problem is discussed here.

There is comprehensive astrophysical literature devoted to diffusion of ions in dense stellar matter. The specific feature of this diffusion is the long-ranged Coulomb interaction between ions. In this respect the diffusion of ions has much in common with the diffusion of particles interacting via a Yukawa potential with sufficiently large screening length. The physics of diffusion has many aspects. One can study different types of diffusion coefficients. Most often considered are self-diffusion coefficients  $D_{ii}$  and, somewhat less often, but more important, interdiffusion coefficients  $D_{ij}$ , which enter the expressions for the diffusion currents. Here,  $i, j = 1, 2, \dots$  enumerate ion species in a multicomponent plasma (MCP). In a one-component plasma (OCP) of ions there is only one self-diffusion coefficient  $D_1$ . Note that a self-diffusion coefficient  $D_{ii}$  in MCP should not be confused with a self-diffusion coefficient  $D_1$  in OCP. One can further consider weak or strong Coulomb coupling, classical or quantum ion motion, the presence of a magnetic field, degenerate or non-degenerate electrons, etc. Diffusion is studied with different techniques such as the Chapman-Enskog approach, Green-Kubo relations, molecular dynamics (MD) simulations, and effective potential method, as well

as other methods and their combinations. Some of these cases and methods are discussed below in more detail.

We mainly focus on the inter-diffusion of ions in binary ionic mixtures (BIMs) which form either Boltzmann gas or a strongly coupled Coulomb liquid. The ions are assumed to be fully ionized and the electrons strongly degenerate (although these restrictions are not very important). The diffusion in a gas is a classical issue, well studied and described in well-known monographs [17, 18]; the diffusion in liquid is less elaborated. Our aim will be to provide a unified treatment of the diffusion coefficients in ion gas and liquid and to present the results in a form convenient for using in numerical simulations of ion diffusion and related phenomena. In a BIM, there is one independent interdiffusion coefficient  $D_{12} = D_{21}$  and two self-diffusion coefficients  $D_{11}$  and  $D_{22}$ .

Weak Coulomb coupling means that the ions constitute almost ideal gas. They are moving more or less freely and diffuse due to relatively weak Coulomb collisions with neighboring ions. The diffusion coefficients in this limit are usually expressed through a Coulomb logarithm  $\Lambda$ , which can be estimated as the logarithm of the large ratio of the maximum to minimum impact parameters of colliding ions. Calculations are done using the classical theory of diffusion in rarefied gases (see Refs. [17, 18]). In astrophysical literature, this theory is often called the Chapman-Salpeter theory (meaning the application of the general theory to diffusion due to Coulomb interaction). Early astrophysical publications based on this theory are cited, for instance, in Ref. [19]. One can further consider the classical and quantum limits in ion-ion scattering (note that the motion of ions is always classical at weak coupling, quantum effects can emerge only in scattering events). In the classical limit, the minimum impact parameter in the expression for  $\Lambda$  is determined by the classical distance of the closest approach of colliding ions. In the quantum limit the minimum impact parameter is determined by the de Broglie wavelengths of ions. One can also consider the cases of non-degenerate and degenerate electrons. In the latter case the electrons produce much weaker screening of the Coulomb interaction (i.e., contribute much less to the maximum impact

parameter) than in the former case. We will focus on the classical scattering limit in the presence of strongly degenerate electrons.

When the coupling becomes stronger, the ratio of the maximum to minimum impact parameters decreases reducing the Coulomb logarithm. At intermediate couplings the Coulomb logarithm becomes  $\Lambda \sim 1$ , and the diffusion coefficients  $D \sim a^2 \omega_p$ , where  $a$  is a typical inter-ion distance and  $\omega_p$  is the ion plasma frequency (see Sec. III). Characteristic ion-ion collision frequencies become comparable to  $\sim \omega_p$ , and typical ion mean free paths are  $\sim a$ .

At strong coupling the ions are mostly confined (caged) in their local potential wells (within respective Wigner-Seitz cells) and constitute either a Coulomb liquid or Coulomb crystal. Thus, the ions mainly oscillate around (quasi-) equilibrium positions and diffuse through thermally activated jumps from one position to another (neighboring) one. The first experimental observations of the caging effect in relaxation of strongly coupled plasmas were made by Bannasch et al. [20]. Here one can distinguish the cases of classical (the temperature  $T \gtrsim T_p$ ) and quantum ( $T \lesssim T_p$ ) ion motion (where  $T_p = \hbar \omega_p / k_B$  is the ion plasma temperature that is close to the Debye temperature, with  $k_B$  being the Boltzmann constant). In the quantum case collective oscillations (plasmons) play an important role. As for electrons, one can study the cases of a rigid (incompressible) electron background or weakly polarizable background. The latter case is similar to the case of ions interacting via Yukawa potentials (with sufficiently large screening length). We consider the diffusion in Coulomb liquid neglecting quantum effects but taking into account both cases of rigid and slightly polarizable electron background. These cases give essentially the same results.

A semianalytic consideration of weak coupling was developed by Fontaine and Michaud [21] who provided the expressions for  $D_{ij}$  through a Coulomb logarithm and developed a computer code for calculating  $D_{ij}$ . The authors considered the cases of quantum and classical minimum impact parameters in the Coulomb logarithm and introduced the resistance coefficients  $K_{ij}$  (that determine the “friction forces” inversely proportional to  $D_{ij}$ ). Their results were extended and used by Iben and MacDonald [5] (in the case of weak coupling) who simulated the evolution of  $^{12}\text{C} - ^{16}\text{O}$  white dwarfs.

Paquette et al. [19] calculated binary diffusion coefficients at weak and moderate couplings using the Chapman-Enskog (Chapman-Spitzer) formalism with a statically screened Coulomb potential. The authors presented accurate analytic fits of collision integrals (tabulated spline coefficients). Their results are applicable as long as Coulomb coupling is not very strong. They discussed also earlier MD calculations of the self-diffusion coefficient at strong coupling.

Pioneering MD calculations of the self-diffusion coefficient  $D_1$  in OCP were performed in 1975 by Hansen et al. [22]. For the ion coupling parameter  $\Gamma > 1$  (defined in

Sec. II) they proposed the fit

$$D_1^* = D_1 / (\omega_p a^2) \approx 2.95 \Gamma^{-4/3}. \quad (1)$$

Hansen et al. [23] carried out MD calculations of  $D_{12}$ ,  $D_{11}$ , and  $D_{22}$  in BIMs in the regime of intermediate and strong couplings. They presented the approximate relation [their Eq. (23)] between the inter- and self-diffusion coefficients,

$$D_{12} \approx x_2 D_{11} + x_1 D_{22}. \quad (2)$$

They tabulated  $D_{12}$ ,  $D_{11}$ , and  $D_{22}$  for some coupling strengths and relative fractions of ions ( $x_1$  and  $x_2 = 1 - x_1$ ) in the  $^1\text{H} - ^4\text{He}$  mixture.

Boercker and Pollock [24] performed MD and advanced kinetic theory calculations of the interdiffusion coefficients in BIMs for strong and weak couplings. The results were in good agreement with previous studies. Robbins et al. [25] considered self-diffusion in OCP using MD of Yukawa systems. Rosenfeld et al. [26] performed MD calculations of BIMs for wide ranges of  $m_2/m_1$  and  $Z_2/Z_1$  (ion mass and charge ratios) at strong, moderate and weak coupling in Coulomb plasmas and in Yukawa systems; they studied self-diffusion and inter-diffusion, and emphasized close relation between these systems and the systems of hard spheres.

Ohta and Hamaguchi [27] did extensive MD calculations of the self-diffusion coefficient in OCP Yukawa systems. They used the Green-Kubo relation and the ordinary space diffusion formula to determine  $D_1$  (and the results converge). They tabulated the computed values of  $D_1^* = D_1 / (\omega_p a^2)$  and approximated  $D_1^*$  by the expression

$$D_1^* = \alpha (T^* - 1)^\beta + \gamma, \quad (3)$$

where  $T^* = T/T_m$ , and  $T_m$  is the melting temperature. They presented the fit parameters  $\alpha$ ,  $\beta$ , and  $\gamma$  as functions of the screening parameter in the Yukawa potential and obtained good agreement with the results for Coulomb systems in the cases of large screening lengths in the Yukawa potentials.

Daligault and Murillo [28] performed MD calculations of the self-diffusion coefficient in OCP using a semiempirical potential and fitted the results by Eq. (3) with  $\gamma = 0.028$ ,  $\alpha = 0.00525$ , and  $\beta = 1.154$ . As the next step Daligault [29] analyzed liquid dynamics in a strongly coupled OCP and concluded that although dynamical behavior of ions (with long-range Coulomb interaction) at strong coupling changed from almost free particle motion to the caging regime, the universal laws or ordinary liquids with short-range interaction remained valid there.

Hughto et al. [30] performed MD calculations of the self-diffusion coefficient of  $^{22}\text{Ne}$  in a mixture of many ion species at strong coupling. They presented an original fit [their Eq. (8)] for  $D_{ii}/D_1$  (a combination of exponents and powers of  $\Gamma$ ).

In his next paper Daligault [31] performed MD simulations of self-diffusion in OCP and BIMs at strong coupling and fitted the results by [his Eq. (4)]

$$D^* = \frac{D}{\omega_p a^2} = \frac{A}{\Gamma} \exp(-B\Gamma), \quad (4)$$

which would be appropriate to the regime of caging and thermally activated jumps ( $A$  and  $B$  being some fit parameters). He considers previous fits at strong coupling [like Eq. (3)] as less physical. In addition, he used standard Chapman-Spitzer results at weak coupling and emphasized very good agreement of MD and Chapman-Spitzer approaches at intermediate coupling. Later Daligault [32] suggested similar ideas for Yukawa OCP systems.

As the next step Khrapak [33] considered the self-diffusion coefficient in OCP. He used the standard Chapman-Spitzer theory at weak coupling and results of MD calculations by different authors at strong coupling. Based on those results he suggested a simple and convenient analytic approximation, which reproduced the cases of weak and strong couplings, by introducing a generalized Coulomb logarithm  $\Lambda_{\text{eff}}$ .

Finally, quite recently Baalrud and Daligault [34] put forward the idea that the cases of weak and strong coupling can be described within the same formalism of the effective binary interaction potential and traditional Chapman-Enskog theory (even at strong Coulomb coupling!). They constructed some examples of the effective potential inferred from radial distribution functions of ions  $g(r)$ ; these functions were computed via the hypernetted chain (HNC) approach. The effective potential allows one not only to account for the screening effects (this can be done by employing the screened Coulomb potential), but also take into account even strong correlations between the ions. This method treats the screening and correlation effects self-consistently; no “external” screening lengths are involved. The authors compared the self-diffusion coefficients in OCP calculated by different methods (their Fig. 2) and emphasized the importance of expressing the diffusion coefficients through generalized Coulomb logarithms. We will follow this approach extending it to BIMs.

For the completeness of our consideration let us mention some others methods which have also been used to calculate diffusion coefficients in simulations of some phenomena in dense stars.

Bildsten and Hall [7] proposed to employ the self-diffusion coefficient  $D_1$  to study  $^{22}\text{Ne}$  settling in white dwarfs (at strong coupling). They tried two forms of  $D_1$ . First, they took  $D_1$  using the Stokes-Einstein relation for a particle of radius  $a_p$  (taken to be the radius of the ion sphere for  $^{22}\text{Ne}$ ) moving in a fluid with viscosity  $\eta$  obtained from fits to the results of MD simulations. This method is suitable for inter-diffusion of trace ions of one species in BIMs. Second, the authors used  $D_1$  obtained in Ref. [22]. They found that the values of  $D_1$  estimated in these two ways were close and led to the same results.

Deloye and Bildsten [8] compared the same two different forms of self-diffusion coefficients at strong coupling to study the  $^{22}\text{Ne}$  settling in white dwarfs. In addition, they took into account computational uncertainties of  $\eta$  and obtained that these uncertainties did not affect noticeably  $D_1$ . They suggested using  $D_1$  taken from Ref. [22] in modeling diffusion processes.

Peng et al. [35] simulated sedimentation and x-ray bursts in neutron stars. In their Appendix they described the resistance coefficients and associated diffusion coefficients. They proposed piece-like interpolation of weak coupling and strong coupling cases. They considered weak coupling following Fontaine and Michaud [36] and strong coupling following Ref. [22].

Although we do not study diffusion in Coulomb crystals let us mention that the problem was investigated by Hugtto et al. [37] using MD with the natural result that this diffusion is strongly suppressed in comparison with that in Coulomb liquid.

It is also worth to mention some papers devoted to diffusion in magnetized Coulomb plasmas. For instance, Bernu [38] calculated the self-diffusion coefficient in OCP with a constant uniform magnetic field  $\mathbf{B}$ . Much later Ranganathan et al. [39] repeated MD calculations of self-diffusion in OCP in a magnetic field. They obtained two self-diffusion coefficients,  $D_{\parallel}$  and  $D_{\perp}$ , along and across  $\mathbf{B}$ . Both coefficients decrease with increasing  $B$ , and  $D_{\perp} < D_{\parallel}$ .

## II. HNC CALCULATION OF EFFECTIVE POTENTIAL

Consider a classical (quantum effects neglected) non-magnetized binary ionic mixture (BIM), which consists of two ion species and neutralizing rigid electron background [40]. An assumption of the rigid electron background allows us to factorize out the electrons while calculating inter-ionic diffusion [16]. Let  $n_j$ ,  $A_j$ , and  $Z_j$  be, respectively, the number density, mass, and charge numbers of ion species  $j = 1$  and  $2$ . For certainty, we set  $Z_1 < Z_2$ . Let  $n = n_1 + n_2$  denote the overall ion number density and  $x_j = n_j/n$  the fractional number of ions  $j$  (with  $x_1 + x_2 = 1$ ). Then we can define the mean value  $\bar{f}$  of any quantity  $f_j$  in a BIM as  $\bar{f} = x_1 f_1 + x_2 f_2$ . In the following (unless the contrary is indicated) lengths are measured in the units of the ion-sphere radius,

$$a = \left( \frac{3}{4\pi n} \right)^{\frac{1}{3}}, \quad (5)$$

and all potentials in units of  $k_B T/e$  ( $e$  being the elementary charge).

A state of the BIM is defined by ion charge and mass numbers and by two dimensionless parameters, the fractional number  $x \equiv x_1$  of ions 1, and the Coulomb cou-

pling parameter  $\Gamma_0$  (see Refs. [23, 40]),

$$\Gamma_0 = \frac{e^2}{ak_B T}. \quad (6)$$

We can also introduce the Coulomb coupling parameter for each ion species (see, e.g., Ref. [41]),

$$\Gamma_j = \frac{Z_j^2 e^2}{a_j k_B T} = \frac{Z_j^{\frac{5}{3}} e^2}{a_e k_B T}, \quad (7)$$

where  $a_e = (3/4\pi n_e)^{1/3}$  is the electron-sphere radius,  $a_j = a_e Z_j^{1/3}$  is the ion sphere radius of species  $j$ , and  $n_e = Z_1 n_1 + Z_2 n_2 = \bar{Z} n$  is the electron number density.

Furthermore, it is convenient to introduce the mean ion coupling parameter  $\bar{\Gamma} = x_1 \Gamma_1 + x_2 \Gamma_2$ , which can be expressed as

$$\bar{\Gamma} = \Gamma_0 \bar{Z}^{\frac{2}{3}} \bar{Z}^{\frac{1}{3}}, \quad (8)$$

and which reduces to  $\bar{\Gamma} = \Gamma_0 \bar{Z}^2$  in the case of OCP.

Let  $g_{ij}(r)$ ,  $h_{ij}(r)$ , and  $c_{ij}(r)$  ( $i, j = 1, 2$ ) be the radial distribution functions (RDFs), the total and direct correlation functions, respectively (as detailed, e.g., in Ref. [42]). All these functions are symmetric [i.e.  $g_{ij}(r) = g_{ji}(r)$ ], and  $h_{ij}(r) = g_{ij}(r) - 1$ . The effective potential  $\Phi(r)$  in OCP is introduced by the relation  $g(r) = \exp[-\Phi(r)]$  [34, 42]. The extension of this relation to the BIM case is straightforward,

$$g_{ij}(r) = \exp[-\Phi_{ij}(r)]. \quad (9)$$

One primarily needs  $\Phi_{12}(r)$  for calculating the interdiffusion coefficient.

Generally, all these functions cannot be calculated analytically. We calculate them by the HNC method, which is known to be sufficiently accurate (as detailed in Sec. IV) and relatively simple (e.g., Refs. [40, 43, 44]). Let us outline this method to simplify the reading of this paper. It consists in solving together the equations of two types, the Ornstein-Zernike equations relating direct and total correlation functions and the HNC closure relations. Since the equations are used in Fourier space, we define the dimensionless Fourier transform as

$$\hat{f}(k) = \frac{4\pi}{k} \int_0^{+\infty} f(r) r \sin(kr) dr \quad (10)$$

(wave number  $k$  is measured in units of  $1/a$ ), and its inverse as

$$f(r) = \frac{1}{2\pi^2 r} \int_0^{+\infty} \hat{f}(k) k \sin(kr) dk. \quad (11)$$

Then the Ornstein-Zernike relations are readily written as [40],

$$\hat{h}_{ij}(k) = \hat{c}_{ij}(k) + \frac{3}{4\pi} \sum_{q=1}^2 x_q \hat{h}_{iq}(k) \hat{c}_{qj}(k), \quad (12)$$

and the HNC closure is

$$g_{ij}(r) = h_{ij}(r) + 1 = \exp[h_{ij}(r) - c_{ij}(r) - \phi_{ij}(r)], \quad (13)$$

$\phi_{ij}(r)$  being the bare Coulomb interaction,

$$\phi_{ij}(r) = \frac{Z_i Z_j \Gamma_0}{r}. \quad (14)$$

Equations (12) and (13) form a closed set of six equations for  $h_{ij}$  and  $c_{ij}$ , but they cannot be solved directly due to the long-range nature of the Coulomb potential. For OCP this problem was circumvented by Springer et al. [43] and Ng [44] by introducing short-ranged potentials and correlation functions. A similar method was used by Hansen et al. [40] for BIMs. Let us outline this method here for the sake of completeness.

In our case the total correlation functions  $h_{ij}(r)$  are short-ranged and the direct correlation functions have the asymptotes [40, 43, 44]

$$\lim_{r \rightarrow \infty} c_{ij}(r) = -\phi_{ij}(r). \quad (15)$$

Let us introduce a quantity

$$\gamma_{ij}(r) = h_{ij}(r) - c_{ij}(r) \quad (16)$$

which has the asymptotic property

$$\lim_{r \rightarrow \infty} \gamma_{ij}(r) = \phi_{ij}(r). \quad (17)$$

Then we define the short-range ( $s$ ) correlation functions and potentials,

$$\gamma_{ij}^{(s)}(r) = \gamma_{ij}(r) - \phi_{ij}^{(l)}(r), \quad (18)$$

$$c_{ij}^{(s)}(r) = c_{ij}(r) + \phi_{ij}^{(l)}(r), \quad (19)$$

$$\phi_{ij}^{(s)}(r) = \phi_{ij}(r) - \phi_{ij}^{(l)}(r). \quad (20)$$

The long-range ( $l$ ) functions  $\phi_{ij}^{(l)}(r)$  have to satisfy two conditions, (1) possess the same asymptotes as  $\phi_{ij}(r)$  at  $r \rightarrow \infty$  and (2) be regular at  $r = 0$ . Otherwise, they are arbitrary. Following Ng [44], we choose

$$\phi_{ij}^{(l)}(r) = \frac{Z_i Z_j \Gamma_0}{r} \operatorname{erf}(\alpha r), \quad (21)$$

with  $\alpha = 1.1$ ; its Fourier transform in Eq. (12) is

$$\hat{\phi}_{ij}^{(l)}(k) = \frac{4\pi Z_i Z_j \Gamma_0}{k^2} \exp\left(-\frac{k^2}{4\alpha^2}\right). \quad (22)$$

Now we rewrite Eqs. (12) and (13) in terms of short-ranged correlation functions and potentials,

$$\begin{aligned} \hat{\gamma}_{ij}^{(s)}(k) + \hat{\phi}_{ij}^{(l)}(k) &= \frac{3}{4\pi} \sum_{q=1}^2 x_q \left[ \hat{\gamma}_{iq}^{(s)}(k) + \hat{c}_{iq}^{(s)}(k) \right] \\ &\times \left[ \hat{c}_{qj}^{(s)}(k) - \hat{\phi}_{qj}^{(l)}(k) \right], \end{aligned} \quad (23)$$

$$g_{ij}(r) = \exp[\gamma_{ij}^{(s)}(r) - \phi_{ij}^{(s)}(r)], \quad (24)$$

$$c_{ij}^{(s)}(r) = g_{ij}(r) - \gamma_{ij}^{(s)}(r) - 1. \quad (25)$$



This system can be solved iteratively starting with a guess for  $c_{ij}^{(s)}(r)$ . Before that the functions  $\hat{\gamma}_{ij}^{(s)}(k)$  should be explicitly expressed from Eqs. (23). As Eqs. (23) are linear with respect to  $\hat{\gamma}_{ij}^{(s)}(k)$ , they can be solved analytically once and for all. We will not write here the resulting formulas because they are inconveniently large and their derivation is obvious. Points  $k = 0$  and  $r = 0$  require special consideration because these values cannot be substituted in Eqs. (23) and (24) due to singularities in  $\hat{\phi}_{ij}^{(l)}(k)$  and  $\phi_{ij}^{(s)}(r)$ , respectively. The problem is dealt with as following. First, the values of  $\hat{\gamma}_{ij}^{(s)}(0)$  and  $g_{ij}(0)$  are calculated separately,

$$\begin{aligned} g_{ij}(0) &= 0, \quad \hat{\gamma}_{11}^{(s)}(0) = -\frac{4\pi}{3x_1} - \hat{c}_{11}^{(s)}(0), \\ \hat{\gamma}_{12}^{(s)}(0) &= -\hat{c}_{12}^{(s)}(0), \quad \hat{\gamma}_{22}^{(s)}(0) = -\frac{4\pi}{3x_2} - \hat{c}_{22}^{(s)}(0) \end{aligned} \quad (26)$$

$[\hat{\gamma}_{ij}^{(s)}(0)$  being a  $k \rightarrow 0$  limit of the solutions of Eqs. (23)]. Second, Fourier and inverse Fourier transforms are rewritten to handle

$$\begin{aligned} \hat{f}(0) &= 4\pi \int_0^{+\infty} f(r)r^2 dr, \\ f(0) &= \frac{1}{2\pi^2} \int_0^{+\infty} \hat{f}(k)k^2 dk. \end{aligned} \quad (27)$$

Numerical calculations were performed on a mesh of  $N_p = 2049$  points running from 0 to  $r_{\max}$  and from 0 to  $k_{\max}$ ;  $r_{\max}$  was taken to be 80 (other values for  $N_p$  and  $r_{\max}$  were also taken to check the stability of numerical procedures);  $k_{\max}$  was computed from the standard relation

$$\begin{aligned} \Delta r &= \frac{r_{\max}}{N_p - 1}, \quad \Delta k = \frac{\pi}{(N_p - 1) \Delta r}, \\ k_{\max} &= (N_p - 1) \Delta k. \end{aligned} \quad (28)$$

Fourier integrals were discretized on a mesh using Simpson's rule (intermediate points were calculated via cubic spline interpolation) and processed by means of appropriate fast Fourier transform. A convergence criterion for iterative process was taken to be

$$\sqrt{\int_0^{r_{\max}} \left( g_{22}^{(q)}(r) - g_{22}^{(q-1)}(r) \right)^2 dr} < 10^{-7}, \quad (29)$$

because  $g_{22}$  converges slower than  $g_{12}$  or  $g_{11}$  (here  $q$  is the iteration number).

After the computations have been completed, the accuracy of our results has been checked by comparing the excess (Coulomb) potential energy with the results of Ref. [40]. The agreement has been found to be quite satisfactory (energies have been reproduced up to five to six significant digits).

The examples of HNC results for a mixture of  $^1\text{H}$  and  $^{12}\text{C}$  ( $x_1 = 0.3$ ,  $x_2 = 0.7$ ) are presented in Figs. 1 and 2.

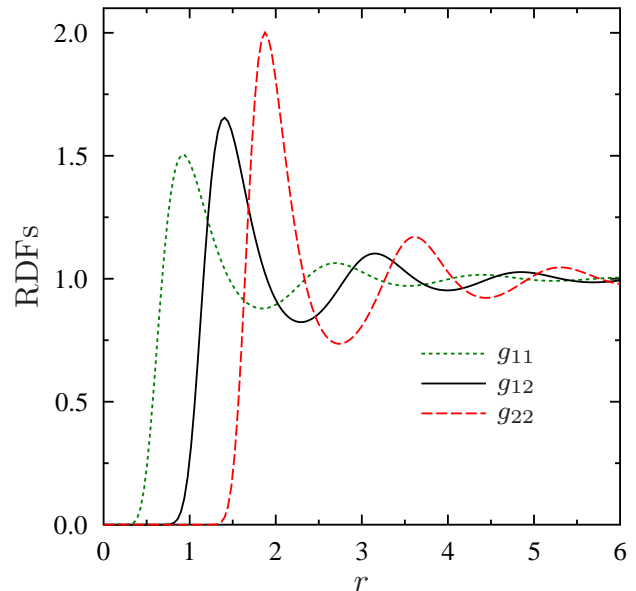


FIG. 1. (Color online) Radial distribution functions for a mixture composed of 30%  $^1\text{H}$  and 70%  $^{12}\text{C}$  (by numbers), with  $\Gamma_0 = 5$  ( $\bar{\Gamma} \approx 117$ ).

### III. DIFFUSION COEFFICIENTS

The standard Chapman-Enskog procedure gives the following leading order approximation to the interdiffusion coefficient in a binary mixture [17, 18] (here in ordinary CGS units):

$$D_{12} = \frac{3}{16} \frac{k_B T}{\mu n} \frac{1}{\tilde{\Omega}_{12}^{(1,1)}}, \quad (30)$$

where  $\mu = m_1 m_2 / (m_1 + m_2)$  is a reduced mass of colliding ions, and  $\tilde{\Omega}$  is a collisional integral defined below. The second order approximation to  $D_{12}$  will be outlined in the next section.

Let us introduce ‘‘hydrodynamic’’ plasma frequency for a mixture (e.g., Ref. [23]):

$$\omega_p = \sqrt{\frac{4\pi n \bar{Z}^2 e^2}{\bar{A} m_0}}, \quad (31)$$

$m_0$  being the atomic mass unit. Let us express the interdiffusion coefficient in units of  $\omega_p a^2$  through a dimensionless collisional integral,

$$D_{12}^* = \frac{D_{12}}{\omega_p a^2} = \frac{\pi^{\frac{3}{2}}}{2\sqrt{6}} \frac{1}{\sqrt{\Gamma_0}} \sqrt{\frac{\bar{A}(A_1 + A_2)}{\bar{Z}^2 A_1 A_2}} \frac{1}{\Omega_{12}^{(1,1)}}. \quad (32)$$

Dimensionless collisional integrals are defined as (see,

TABLE I. Fit parameters in Eq. (39) as well as rms and maximum fit errors. The last column contains values of  $x_1$  and  $\Gamma_0$  at which maximum fit error is achieved

Mixture	$p_1$	$p_2$	$p_3$	$p_4$	$p_5$	$\delta_{\text{rms}}, \%$	$\delta_{\text{max}}, \%$	$(x_1, \Gamma_0)_{\text{max}}$
$^1\text{H} - ^4\text{He}$	$7.43 \times 10^{-2}$	$-1.13 \times 10^{-2}$	$1.72 \times 10^{-1}$	$8.57 \times 10^{-2}$	1.45	3.1	10	(0.7, 0.4)
$^1\text{H} - ^{12}\text{C}$	$3.80 \times 10^{-2}$	$6.57 \times 10^{-3}$	$2.52 \times 10^{-2}$	$1.39 \times 10^{-1}$	1.34	5.6	18	(0.99, 0.729)
$^4\text{He} - ^{12}\text{C}$	$7.01 \times 10^{-3}$	$9.08 \times 10^{-4}$	$1.09 \times 10^{-2}$	$1.17 \times 10^{-1}$	1.41	4.0	13	(0.9, 5.785)
$^{12}\text{C} - ^{16}\text{O}$	$9.95 \times 10^{-5}$	$-6.35 \times 10^{-6}$	$1.61 \times 10^{-3}$	$3.96 \times 10^{-2}$	1.48	2.6	10	(0.9, 0.015)
$^{16}\text{O} - ^{79}\text{Se}$	$7.22 \times 10^{-5}$	$5.00 \times 10^{-5}$	$1.14 \times 10^{-4}$	$1.33 \times 10^{-1}$	1.38	4.1	16	(0.9, 0.187)

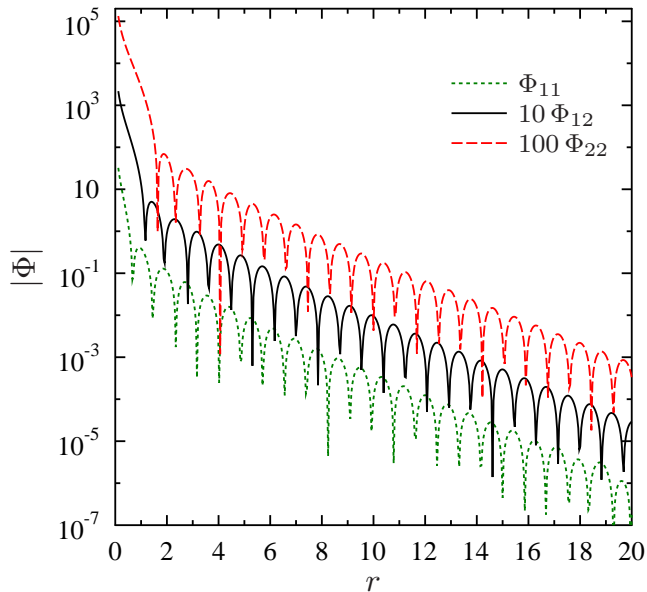


FIG. 2. (Color online) Absolute values of effective potentials for the same mixture of  $^1\text{H}$  and  $^{12}\text{C}$  as in Fig. 1. For a better visualization,  $\Phi_{12}$  is multiplied by 10 and  $\Phi_{22}$  by 100.

e.g., Refs. [19] and [45])

$$\Omega_{12}^{(\xi, \zeta)} = \int_0^\infty \exp(-y^2) y^{2\zeta+3} Q_{12}^{(\xi)}(y) dy, \quad (33)$$

$$Q_{12}^{(\xi)}(u) = 2\pi \int_0^\infty [1 - \cos^\xi(\chi_{12}(b, u))] b db, \quad (34)$$

$$\chi_{12}(b, u) = \left| \pi - 2b \int_{r_{12}^{\min}}^\infty \frac{dr}{r^2 \sqrt{1 - \frac{b^2}{r^2} - \frac{\phi_{12}}{u^2}}} \right|, \quad (35)$$

where  $\chi_{12}$  is the classical scattering angle,  $b$  is the impact parameter,  $\phi_{12}$  the interaction potential between particles 1 and 2,  $u$  is the dimensionless relative velocity (at infinity; in units of  $\sqrt{2k_B T/\mu}$ ),  $r_{12}^{\min}$  is the distance of the closest approach [i.e. maximum root of the denominator in the integrand (35)].

For a weakly coupled (WC) BIM ( $\bar{\Gamma} \ll 1$ ), the diffusion coefficient (32) can be calculated analytically (e.g., Refs.

[17, 18]):

$$D_{12}^{*(\text{WC})} = \sqrt{\frac{\pi}{6}} \frac{1}{\Gamma_0^{\frac{5}{2}}} \sqrt{\frac{\bar{A}(A_1 + A_2)}{Z^2 A_1 A_2}} \frac{1}{Z_1^2 Z_2^2 \Lambda^{(\text{WC})}}, \quad (36)$$

where  $\Lambda^{(\text{WC})}$  is a ‘‘classical’’ Coulomb logarithm for a weakly coupled plasma,

$$\Lambda^{(\text{WC})} = \ln \left( \frac{1}{\sqrt{3} \Gamma_0^{\frac{3}{2}} Z_1 Z_2 \sqrt{Z^2}} \right). \quad (37)$$

Now the algorithm for computing  $D_{12}^*$  at arbitrary coupling is straightforward. First, we calculate RDFs using HNC method described in Sec. II. Second, we find effective potential  $\Phi_{12}$  from Eq. (9) and substitute it instead of  $\phi_{12}$  in the integral (35). Then we calculate  $D_{12}^*$  from Eqs. (32), (33), and (34).

We have performed such calculations of the interdiffusion coefficients for  $^1\text{H} - ^4\text{He}$ ,  $^1\text{H} - ^{12}\text{C}$ ,  $^4\text{He} - ^{12}\text{C}$ ,  $^{12}\text{C} - ^{16}\text{O}$ , and  $^{16}\text{O} - ^{79}\text{Se}$  mixtures for a variety of values of  $\Gamma_0$  and  $x_1$ . We could have easily considered other BIMs if necessary. The easiest way to present these data is to fit the effective Coulomb logarithm by an analytic expression. We have calculated  $D_{12}^*$  and then  $\Lambda_{\text{eff}}$  using the expression:

$$\Lambda_{\text{eff}} = \sqrt{\frac{\pi}{6}} \frac{1}{D_{12}^* Z_1^2 Z_2^2 \Gamma_0^{\frac{5}{2}}} \sqrt{\frac{\bar{A}(A_1 + A_2)}{Z^2 A_1 A_2}}. \quad (38)$$

Thus,  $\Lambda_{\text{eff}}$  coincides with  $\Lambda^{(\text{WC})}$ , Eq. (36), in the weak coupling limit. The examples of  $\Lambda_{\text{eff}}$  for  $^1\text{H} - ^{12}\text{C}$  mixture are presented in Fig. 3.

Fitting  $\Lambda_{\text{eff}}$  instead of  $D_{12}^*$  is more convenient because  $\Lambda_{\text{eff}}$  is expected to be relatively weakly dependent on plasma parameters (particularly on relative number density  $x_1$ ). We propose the fit

$$\Lambda_{\text{eff}}(\Gamma_0, x_1) = \ln \left( 1 + \frac{p_1 x_1^2 + p_2 x_2^2 + p_3}{\Gamma_0^{p_4 x_1 + p_5}} \right), \quad (39)$$

which contains five parameters  $p_1, \dots, p_5$ . These parameters are presented in Table I along with the root mean square (rms) relative deviation,  $\delta_{\text{rms}}$ , and the maximum relative fit errors,  $\delta_{\text{max}}$ . The  $x_1$  mesh points have been taken as  $x_1 = 0.01, 0.1, 0.2, 0.3, \dots, 0.9, 0.99$ . The  $\Gamma_0$

TABLE II.  $\Gamma_0$  mesh points used for computing and fitting  $\Lambda_{\text{eff}}$ . For each BIM the points have been distributed within three ranges I, II and III;  $\Delta^+$  and  $\Delta^\times$  determine the distances between neighboring points as described in the text. Lower bounds of each range are exact, upper bounds are rounded up

Mixture	$\Gamma_0$ range I	$\Gamma_0$ range II	$\Gamma_0$ range III
$^1\text{H} - ^4\text{He}$	$[10^{-4}, 0.05], \Delta^+ = 0.002$	$[0.4, 1.6], \Delta^\times = 1.25$	$[1.7, 52], \Delta^\times = 1.3$
$^1\text{H} - ^{12}\text{C}$	$[10^{-4}, 0.01], \Delta^+ = 0.001$	$[0.15, 0.4], \Delta^\times = 1.2$	$[0.4, 6], \Delta^\times = 1.35$
$^4\text{He} - ^{12}\text{C}$	$[10^{-4}, 0.005], \Delta^+ = 3.5 \times 10^{-4}$	$[0.06, 0.2], \Delta^\times = 1.25$	$[0.2, 5.8], \Delta^\times = 1.4$
$^{12}\text{C} - ^{16}\text{O}$	$[10^{-4}, 0.003], \Delta^+ = 10^{-4}$	$[0.015, 0.05], \Delta^\times = 1.35$	$[0.055, 3.2], \Delta^\times = 1.4$
$^{16}\text{O} - ^{79}\text{Se}$	$[10^{-5}, 2.5 \times 10^{-4}], \Delta^+ = 10^{-5}$	$[0.003, 0.01], \Delta^\times = 1.22$	$[0.01, 0.2], \Delta^\times = 1.34$

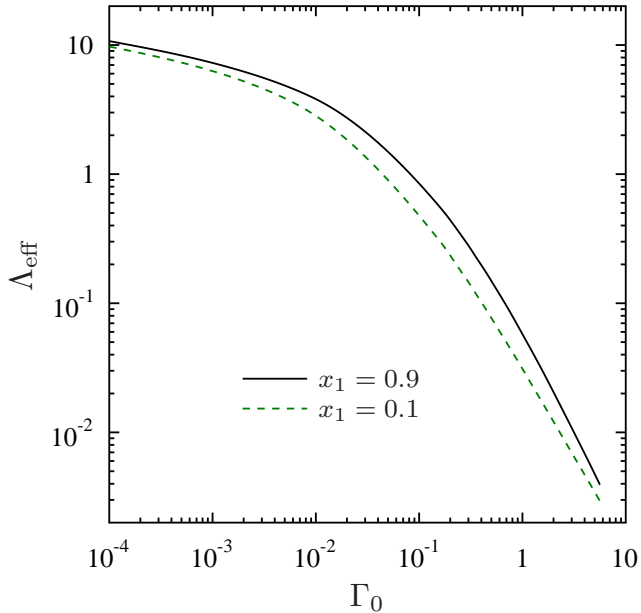


FIG. 3. (Color online) Effective Coulomb logarithm  $\Lambda_{\text{eff}}$  calculated from Eq. (38) for the  $^1\text{H} - ^{12}\text{C}$  mixture. Regions of weak and strong couplings can be clearly seen as well as a transition region between them.

mesh points have been selected differently for each BIM (Table II). For each BIM, the mesh points have been distributed over three ranges of  $\Gamma_0$  labeled as I, II, and III in Table II. These ranges refer to weak, intermediate, and strong Coulomb pairing, respectively (note that the actual strength of Coulomb coupling is determined by  $\bar{\Gamma}$ , not by  $\Gamma_0$ ). In range I the points have been taken equidistant (any next point being larger than the previous one by  $\Delta^+$ ), whereas in ranges II and III logarithmically equidistant (any next point was  $\Delta^\times$  times higher than the previous one).

#### IV. DISCUSSION

Before discussing the results let us make a few remarks.

(1) There is no strict proof for the existence of an effective pair interaction potential which would *entirely* incorporate all many-body effects (correlations) between particles in a strongly coupled Coulomb plasma. Moreover, it seems highly unlikely that such a potential could exist in principle. Nevertheless, the effective potential method seems to be a promising tool for obtaining reasonably accurate solutions of some problems of strongly coupled dense plasmas (see the original work by Baalrud and Daligault [34]).

(2) We use a standard HNC procedure to calculate RDFs. Although some improved HNC techniques have been developed (e.g. Ref. [46]), we consider the accuracy of the standard HNC method sufficient for our purpose. As seen from Fig. 2 of Ref. [34], even using the “exact” RDFs computed via MD simulations makes almost negligible changes to the resulting Chapman-Enskog diffusion coefficient compared to using RDFs obtained via standard HNC method.

(3) Second order Chapman-Enskog approximation to the interdiffusion coefficient in a BIM can be written as [17, 18]

$$[D_{12}^*]_2 = \frac{D_{12}^*}{1 - \Delta}, \quad (40)$$

where

$$\Delta = 5(C - 1)^2 \frac{P_1 \frac{x_1}{x_2} + P_2 \frac{x_2}{x_1} + P_{12}}{Q_1 \frac{x_1}{x_2} + Q_2 \frac{x_2}{x_1} + Q_{12}}, \quad (41)$$

$$P_1 = \left( \frac{A_1}{A_1 + A_2} \right)^3 E_1, \quad P_2 = \left( \frac{A_2}{A_1 + A_2} \right)^3 E_2, \quad (42)$$

$$P_{12} = \frac{3(A_1 - A_2)^2 + 4A_1 A_2 A}{(A_1 + A_2)^2}, \quad (43)$$

$$Q_1 = A_1 E_1 \frac{6A_2^2 + 5A_1^2 - 4A_1^2 B + 8A_1 A_2 A}{(A_1 + A_2)^3}, \quad (44)$$

$$Q_{12} = \frac{3(A_1 - A_2)^2(5 - 4B) + 4A_1 A_2 A(11 - 4B)}{(A_1 + A_2)^2} + \frac{2E_1 E_2 A_1 A_2}{(A_1 + A_2)^2}, \quad (45)$$

TABLE III. Comparison of  $D_{12}^*$  calculated here with MD data and verification of Eq. (48) for  ${}^1\text{H}-{}^4\text{He}$  and  ${}^1\text{H}-{}^{12}\text{C}$  mixtures. The values of  $D_{12}^{*\text{MD}}$  are taken from MD simulations of Hansen et al. [23]. The values  $D_{12}^{*\text{S}}$  are obtained from Eq. (48) with the self-diffusion coefficients calculated by the effective potential method.

${}^1\text{H} - {}^4\text{He}$					${}^1\text{H} - {}^{12}\text{C}$			
$x_1$	$\Gamma_0$	$D_{12}^*$	$D_{12}^{*\text{S}}$	$D_{12}^{*\text{MD}}$	$x_1$	$\Gamma_0$	$D_{12}^*$	$D_{12}^{*\text{S}}$
0.5	0.397	4.20	3.73	3.00	0.2	5.75	0.0572	0.0322
0.5	3.992	0.268	0.230	0.142	0.5	5.75	0.0635	0.0354
0.5	39.738	0.0290	0.0242	0.0109	0.8	5.75	0.0688	0.0445
0.75	40.831	0.0279	0.0235	0.0122				
0.25	40.610	0.0277	0.0237	0.0076				

$$A = \frac{\Omega_{12}^{(2,2)}}{5\Omega_{12}^{(1,1)}}, \quad B = \frac{5\Omega_{12}^{(1,2)} - \Omega_{12}^{(1,3)}}{5\Omega_{12}^{(1,1)}}, \quad C = \frac{2\Omega_{12}^{(1,2)}}{5\Omega_{12}^{(1,1)}}, \quad (46)$$

$$E_j = \frac{\Omega_{jj}^{(2,2)}}{5\Omega_{12}^{(1,1)}} \frac{(A_1 + A_2)^2}{A_1 A_2} \sqrt{\frac{2A_1 A_2}{A_j(A_1 + A_2)}}, \quad j = 1, 2; \quad (47)$$

$Q_2$  is obtained from  $Q_1$  by interchanging indices 1 and 2. Integrals  $\Omega_{jj}^{(2,2)}$  are defined in exactly the same way as  $\Omega_{12}^{(\xi,\zeta)}$  but with  $\Phi_{jj}$  instead of  $\Phi_{12}$ . We have performed calculations of the second-order corrections and found that they do not exceed 5% for the  ${}^1\text{H} - {}^{12}\text{C}$  mixture. For mixtures of more similar ions these corrections are even smaller. Consequently, we have neglected them as the accuracy of the results is limited by the fit errors and by the effective potential method itself.

Unfortunately, there is not very much data available to compare our interdiffusion coefficients with. As seen from Fig. 4 and Table III, the diffusion coefficients  $D_{12}^*$  obtained via the effective potential are systematically larger than the MD results  $D_{12}^{*\text{MD}}$  of Hansen et al. [23], and the difference increases with increasing  $\Gamma_0$ . This is exactly the same behavior as in the original work of Baalrud and Daligault [34] (their Fig. 2) who proposed the effective potential method. We have also compared our data to MD data of Refs. [24, 26] and obtained similar results. This seems to be the consequence of the approximate nature of the effective potential method itself. Since MD data are obtained from first principles, they should have been considered as superior to HNC ones. Nevertheless, the disagreement between the MD and HNC results appears at strong Coulomb coupling where quantum effects in ion motion become important. Unfortunately, the quantum effects are included neither in the MD nor in the HNC schemes we refer to. In this situation, we see no way to check our results with really exact solutions. Therefore, we propose to use the HNC results, which can be obtained quickly. We do not expect that the exact solution, if available, would lead to very different diffusion of ions in liquid BIMs.

Using our (effective potential)  $D_{12}$ , we have also tried to derive an approximate relation similar to (2). Our

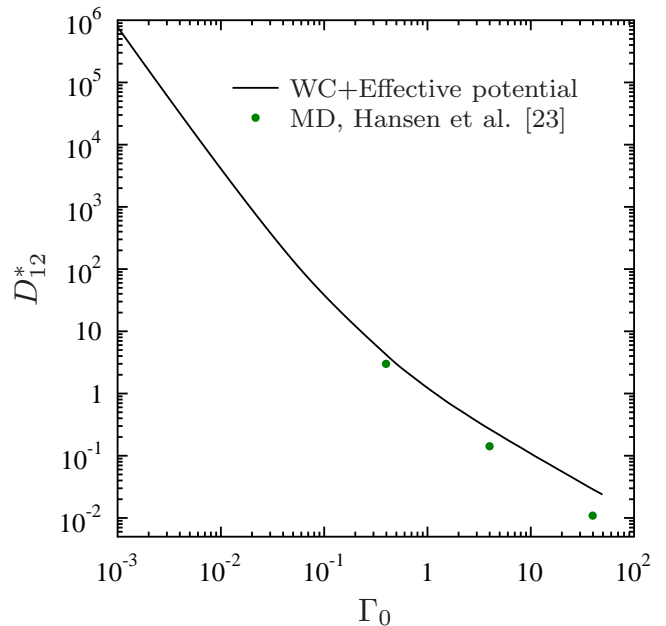


FIG. 4. (Color online). Interdiffusion coefficient  $D_{12}^*$  for  ${}^1\text{H} - {}^4\text{He}$  mixture ( $x_1 = 0.5$ ) and its comparison with MD data of Ref. [23]. Weak, strong and intermediate coupling regions are distinguishable (cf. Fig. 3). Exact values of  $D_{12}^*$  are given in Table III.

best attempt gives  $D_{12} \approx D_{12}^{\text{S}}$ , with

$$D_{12}^{\text{S}}(n, T) \approx x_2 D_1(\tilde{n}_1, T) + x_1 D_2(\tilde{n}_2, T), \quad (48)$$

where  $D_1$  and  $D_2$  are self-diffusion coefficients in “equivalent” OCPs and

$$\tilde{n}_j = \frac{\overline{Z^2}}{Z_j^2} n. \quad (49)$$

Such a choice of  $\tilde{n}_j$  forces the Debye screening length in “equivalent” OCPs to be the same as in the BIM. This resembles the linear mixing rule (see, e.g., Ref. [40]), where “equivalent” OCPs are taken in such a way that they retain the same electron number density as in a BIM



[i.e.  $\tilde{n}_j = (\bar{Z}/Z_j)n$ ]. Equation (48) was initially obtained semiempirically for weakly coupled plasma, but is not greatly violated in the strong coupling regime, despite the fact that the concept of the Debye ion screening length does not apply to strongly coupled plasma. Examples of  $D_{12}^S$  are presented in Table III.

## V. CONCLUSIONS

We have considered interdiffusion coefficients  $D_{12}$  of ions (of two species, 1 and 2) in BIMs under the assumption that the ions constitute either a Boltzmann gas or Coulomb liquid, and the electrons form nearly a uniform background. The problem has been studied for a long time in a number of publications (Sec. I), but a unified practical procedure of calculating many diffusion coefficients important for applications has been absent. The main obstacle consisted in substantial computational difficulties of calculating  $D_{12}$  by rigorous methods like MD in the regime of strong Coulomb coupling.

We have used the method of effective inter-ion potential suggested recently by Baalrud and Daligault [34]. They proposed to determine the effective potential by a reasonably simple HNC scheme and use this potential to evaluate the diffusion coefficient by the standard Chapman-Enskog method. The latter method is known to be strictly valid for rarefied, weakly coupled plasmas, whereas Baalrud and Daligault suggested to apply it in both regimes (gas and liquid). They proved that the method is reasonably accurate for calculating the self-diffusion coefficient of ions in OCP. We have extended their consideration to BIMs and show that the method remains sufficiently accurate for calculating interdiffusion coefficients in BIMs. The combination of two well-elaborated schemes (the HNC scheme for finding the effective potential and the Chapman-Enskog scheme for evaluating kinetic coefficients) makes this method feasible for determining many interdiffusion coefficients of practical importance in BIMs over wide ranges of temperatures and densities.

To demonstrate the efficiency of this method we have calculated  $D_{12}$  for five BIMs ( $^1\text{H}-^4\text{He}$ ,  $^1\text{H}-^{12}\text{C}$ ,  $^4\text{He}-^{12}\text{C}$ ,  $^{12}\text{C}-^{16}\text{O}$ ,  $^{16}\text{O}-^{79}\text{Se}$ ). In analogy with the results of Ref. [33], the diffusion coefficients  $D_{12}$  have been expressed (38) through a generalized Coulomb logarithm  $\Lambda_{\text{eff}}$ . We have approximated all calculated values of  $\Lambda_{\text{eff}}$  by a unified fit formula (39) which contains five fit parameters for each BIM (listed in Table I). In this way we have obtained a unified description of the interdiffusion coefficients for these BIMs. We may easily consider other BIMs if necessary.

Let us stress once more that in the strongly coupled plasma the employed effective potential approach [34] is phenomenological. We expect that our results can be less accurate in this limit than in the limits of weak and intermediate Coulomb couplings. However, when the temperature decreases to the melting temperature  $T_m$ , quantum

effects in ion motion can become important for various properties of the matter (e.g., Ref. [41]). In particular, they can affect diffusion, and the effect has not been studied at all, to the best of our knowledge. In this situation (the quantum effects are neglected anyway) our approach seems reasonable (although the incorporation of quantum effects would be desirable).

Although we have not focused on self-diffusion coefficients in BIMs, we remark that they are most probably calculated by the effective potential method less accurately than the self-diffusion coefficients in OCP [34]. The nature of this phenomenon is not entirely clear. It may be because the calculation of self-diffusion coefficients  $D_{ii}$  for one component in a BIM requires not only  $\Phi_{ii}$ , but also  $\Phi_{ij}$ , whereas, according to Sec. IV, the computation of the interdiffusion coefficient  $D_{ij}$  primarily requires only  $\Phi_{ij}$ . This problem remains to be solved along the basic problem of why the effective potential is reasonably successful in the regime of strong coupling.

Our results (combined with those of Ref. [16]) can be used to study various diffusion processes of ions in the crust of neutron stars and in the cores of white dwarfs (e.g. Refs. [1–10]) as well as in dense Coulomb plasmas of giant and supergiant stars and giant planets. Such diffusion processes can affect thermodynamics and kinetics of dense matter, thermal and chemical evolution of these stars, and their vibrational properties (seismology). The diffusion properties of Coulomb plasmas are also important for dusty plasmas, inertial confinement fusion, etc. (Sec. I).

Numerically, our diffusion coefficients are in reasonable agreement with those obtained by other authors and with different techniques (Sec. I). The main advantage of our results is in simplicity, uniformity, and convenient approximate expressions. Another important advantage is that the effective potential method can be easily generalized for calculating other kinetic properties of strongly coupled Coulomb plasmas, for instance, the diffusion and thermal diffusion coefficients in multicomponent ion mixtures which are needed for applications but which are almost not considered in the literature. However, we should warn the reader once more that the method of an effective potential at strong Coulomb coupling is phenomenological in its essence. It would be important to justify this method and understand the conditions at which it is most accurate. It would be even more important to study diffusion in strongly coupled Coulomb plasmas taking into account quantum effects in ion motions. However, all these difficult issues seem to be beyond the scope of the present investigation.

Although we have a considered rigid (almost incompressible) electron background, the results can be easily generalized to the case of compressible background produced by electrons of any degeneracy and relativity.

## ACKNOWLEDGMENTS

The authors are grateful for the partial support by the State Program “Leading Scientific Schools of Russian

Federation” (grant NSh 294.2014.2). The work of MB has also been partly supported by the Dynasty Foundation, and the work of DY by Russian Foundation for Basic Research (grants Nos. 14-02-00868-a and 13-02-12017-ofi-M) and by “NewCompStar”, COST Action MP1304.

- 
- [1] A. Y. Potekhin, G. Chabrier, and D. G. Yakovlev, *Astron. Astrophys.* **323**, 415 (1997).
- [2] P. Chang and L. Bildsten, *Astrophys. J.* **585**, 464 (2003).
- [3] P. Chang and L. Bildsten, *Astrophys. J.* **605**, 830 (2004).
- [4] P. Chang, L. Bildsten, and P. Arras, *Astrophys. J.* **723**, 719 (2010).
- [5] I. Iben, Jr. and J. MacDonald, *Astrophys. J.* **296**, 540 (1985).
- [6] J. Isern, M. Hernanz, R. Mochkovitch, and E. García-Berro, *Astron. Astrophys.* **241**, L29 (1991).
- [7] L. Bildsten and D. M. Hall, *Astrophys. J. Lett.* **549**, L219 (2001).
- [8] C. J. Deloye and L. Bildsten, *Astrophys. J.* **580**, 1077 (2002).
- [9] L. G. Althaus, E. García-Berro, I. Renedo, J. Isern, A. H. Córscico, and R. D. Rohrmann, *Astrophys. J.* **719**, 612 (2010).
- [10] E. García-Berro, S. Torres, L. G. Althaus, I. Renedo, P. Lorén-Aguilar, A. H. Córscico, R. D. Rohrmann, M. Salaris, and J. Isern, *Nature* **465**, 194 (2010).
- [11] G. Chabrier, D. Saumon, and A. Y. Potekhin, *J. Phys. A* **39**, 4411 (2006).
- [12] O. S. Vaulina, X. G. Koss, Y. V. Khrustalyov, O. F. Petrov, and V. E. Fortov, *Phys. Rev. E* **82**, 056411 (2010).
- [13] S. Atzeni and J. Meyer-ter-Vehn, *The Physics of Inertial Fusion*, vol. 125 (Oxford Univ. Press, Oxford, 2004).
- [14] G. B. Andresen, M. D. Ashkezari, M. Baquero-Ruiz, W. Bertsche, P. D. Bowe, E. Butler, C. L. Cesar, S. Chapman, M. Charlton, J. Fajans, et al., *Phys. Rev. Lett.* **105**, 013003 (2010).
- [15] T. C. Killian, *Science* **316**, 705 (2007).
- [16] M. V. Beznogov and D. G. Yakovlev, *Phys. Rev. Lett.* **111**, 161101 (2013).
- [17] S. Chapman and T. G. Cowling, *The Mathematical Theory of Non-Uniform Gases* (Cambridge Univ. Press, Cambridge, 1952).
- [18] J. O. Hirschfelder, C. F. Curtiss, and R. B. Bird, *Molecular Theory of Gases and Liquids* (Wiley, New York, 1954).
- [19] C. Paquette, C. Pelletier, G. Fontaine, and G. Michaud, *Astrophys. J. Suppl.* **61**, 177 (1986).
- [20] G. Bannasch, J. Castro, P. McQuillen, T. Pohl, and T. C. Killian, *Phys. Rev. Lett.* **109**, 185008 (2012).
- [21] G. Fontaine and G. Michaud, in *IAU Colloq. 53: White Dwarfs and Variable Degenerate Stars*, edited by H. M. van Horn and V. Weidemann (University of Rochester Press, Rochester, 1979), pp. 192–196.
- [22] J. P. Hansen, I. R. McDonald, and E. L. Pollock, *Phys. Rev. A* **11**, 1025 (1975).
- [23] J. P. Hansen, F. Joly, and I. R. McDonald, *Physica A* **132**, 472 (1985).
- [24] D. B. Boercker and E. L. Pollock, *Phys. Rev. A* **36**, 1779 (1987).
- [25] M. O. Robbins, K. Kremer, and G. S. Grest, *J. Chem. Phys.* **88**, 3286 (1988).
- [26] Y. Rosenfeld, E. Nardi, and Z. Zinamon, *Phys. Rev. Lett.* **75**, 2490 (1995).
- [27] H. Ohta and S. Hamaguchi, *Phys. Plasmas* **7**, 4506 (2000).
- [28] J. Daligault and M. S. Murillo, *Phys. Rev. E* **71**, 036408 (2005).
- [29] J. Daligault, *Phys. Rev. Lett.* **96**, 065003 (2006).
- [30] J. Hughto, A. S. Schneider, C. J. Horowitz, and D. K. Berry, *Phys. Rev. E* **82**, 066401 (2010).
- [31] J. Daligault, *Phys. Rev. Lett.* **108**, 225004 (2012).
- [32] J. Daligault, *Phys. Rev. E* **86**, 047401 (2012).
- [33] S. A. Khrapak, *Phys. Plasmas* **20**, 054501 (2013).
- [34] S. D. Baalrud and J. Daligault, *Phys. Rev. Lett.* **110**, 235001 (2013).
- [35] F. Peng, E. F. Brown, and J. W. Truran, *Astrophys. J.* **654**, 1022 (2007).
- [36] G. Fontaine and G. Michaud, *Astrophys. J.* **231**, 826 (1979).
- [37] J. Hughto, A. S. Schneider, C. J. Horowitz, and D. K. Berry, *Phys. Rev. E* **84**, 016401 (2011).
- [38] B. Bernu, *J. Physique Lett.* **42**, 253 (1981).
- [39] S. Ranganathan, R. E. Johnson, and C. E. Woodward, *Phys. Chem. Liq.* **41**, 123-132 (2003).
- [40] J. P. Hansen, G. M. Torrie, and P. Vieillefosse, *Phys. Rev. A* **16**, 2153 (1977).
- [41] P. Haensel, A. Y. Potekhin, and D. G. Yakovlev, *Neutron Stars. 1. Equation of State and Structure*, vol. 326 of *Astrophysics and Space Science Library* (Springer, New York, 2007).
- [42] C. A. Croxton, *Liquid State Physics—A Statistical Mechanical Introduction*, Cambridge Monographs on Physics (Cambridge Univ. Press, Cambridge, 1974).
- [43] J. F. Springer, M. A. Pokrant, and F. A. Stevens, *J. Chem. Phys.* **58**, 4863 (1973).
- [44] K.-C. Ng, *J. Chem. Phys.* **61**, 2680 (1974).
- [45] L. D. Landau and E. M. Lifshitz, *Mechanics* (Butterworth-Heinemann, Oxford, 1976), 3rd ed.
- [46] H. Iyetomi and S. Ichimaru, *Phys. Rev. A* **27**, 3241 (1983).